The Institute of Space and Astronautical Science
Report SP No. 15, March 2003

Simultaneous observation of the faint meteors by the MU radar head echo mode and a high sensitive video camera

By

Masumi NISHIO*, Takuji NAKAMURA†, Toru SATO‡, Shuichi TSUTSUMI‡, Toshitaka TSUDA† and Ken-ichi FUSHIMI*

(1 February 2003)

Abstract: The meteor head echo observation using the MU radar (46.5 MHz, 1 MW), Shigaraki, Japan has been developed since 1998 for Leonid meteor observations. Orbits of faint meteors with +15 magnitude can be measured with a precision of 0.5 degree (Nishimura et al., 2001). Simultaneous optical observation with an ICCD (Image-intensified CCD) video camera was carried out. Instantaneous radar signal intensity and video magnitudes are closely compared by using a time-recording system synchronized to GPS signals. We have found that the light curve and time variation of radar signal intensity compares fairly well in many cases, but quite frequently the radar signal becomes decreased by 10-20 dB quickly without any significant change of video magnitude. This suggests a change of radar scattering mechanism of a meteor head during the flight.

1. INTRODUCTION

A meteoroid is a solid particle which drifts in the solar system, with a diameter ranging from 1 mm to 1 m. However, a smaller meteoroid with a diameter of several mm or less exists in large numbers. The distribution of the orbit and mass are not known well. The geocentric velocity of meteoroids reaches 72 km/s, and therefore care must be taken even for small meteoroids in spacecraft operation, the number of which is huge compared with large meteoroids.

The collision of meteoroid to the earth atmosphere causes heating and luminosity, and ionizes the atmosphere. Such phenomena are observed as meteors. The optical observation of the light of a meteor includes visual observation, photograph observation and TV observation. Optical magnitudes and the mass of meteor measured by these observations have been accumulated abundantly. In the photograph observation using Super-Schmidt camera, meteors with a magnitude down to +3 magnitude can be captured, and meteors down to +9 magnitude

* Faculty of Integrated Arts and Sciences, the University of Tokushima, Tokushima, 770-8502, Japan.
† Radio Science Center for Space and Atmosphere, Kyoto University, Uji, Kyoto, 611-0011, Japan.
‡ Department of Communication and Computer Engineering, Graduate School of Informatics, Kyoto University, Kyoto, 606-8501, Japan.

are observed with LLLTV (Low Light Level TV) observation (Ceplecha et al., 1998). In recent years, observation of a meteor fainter than +9 magnitude has been carried out using the CCD camera with an image-intensifier. On the other hand, the radar observation is able to capture meteors fainter than +10 magnitude. Radars have been used to study activities of shower and sporadic meteors, orbits, distributions and masses. However, among them mass of meteors is difficult to derive because there are unclarified parameters in the relation between radar echo intensity and mass.

In this study, radio scattering and optical magnitude of the faint meteors have been investigated using a precise determination of meteor orbits with the MU radar, in order to estimate the mass of faint meteors which is not sensitive in optical observation from radar observation. Therefore, radar and optical observation have been carried out simultaneously with the MU (Middle and Upper atmosphere) radar and a high sensitive video camera (ICCD camera). Both radar and optical systems are synchronized using GPS (Global Positioning System) satellite signal, which enables to compare instantaneous RCS (radar cross section) and optical magnitude of the meteor head.

2. OBSERVATION

2.1 Optical observation

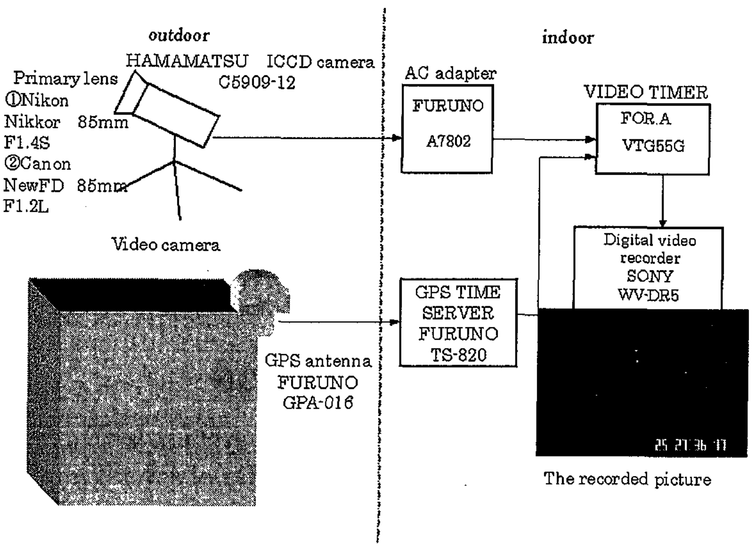

Fig. 1: Outline of optical observation system

Fig. 1 shows an outline of optical observation system. The high sensitive video camera system consists of a primary lens, on ICCD camera unit (C5909-12, Hamamatsu) and a digital video recorder. In the ICCD camera unit, two stages of MCP (Micro Channel Plate) intensifies an image collected by the primary lens. We utilized a Nikon Nikkor 85 mm F1.4S as a primary lens (Lens 1) in our observation during May - November 2001. At around 2:30 'JST' on November 21, 2001, we changed the lens to Cannon NewFD 85 mm F1.2L (Lens 2). The field of view is 6.6 × 8.8 degree in the ICCD camera unit. Data were recorded on DV tapes with

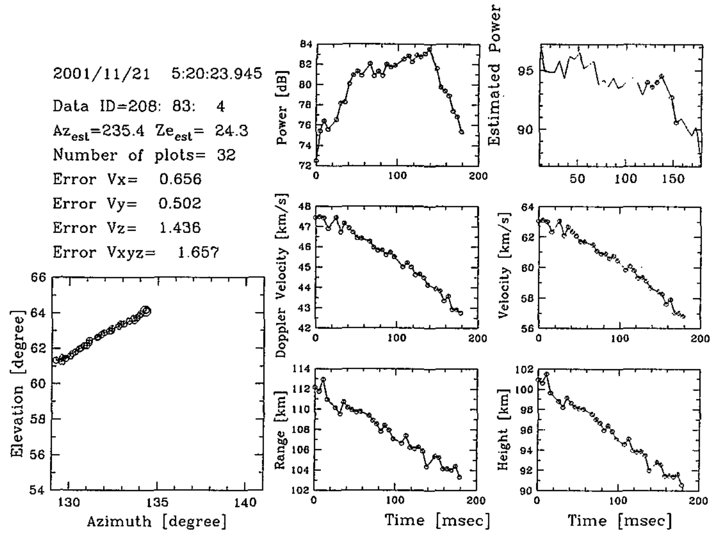

Fig. 2: An example of the radar observation result. The left panel shows tracks of the meteor head in apparent directions observed by the radar. Observed radar echo intensities (antenna gain pattern uncorrected), Doppler velocities, ranges are displayed in the center column (from the top to the bottom). Similarly, radar echo intensities with antenna gain pattern corrected, meteor head velocities, and heights are plotted in the right column.

the standard mode (4.5 hours/tape) by DV format using a video cassette recorder of standard DV.

2.2 Radar observation

The MU radar, located at Shigaraki, Shiga, Japan, utilizes the frequency of 46.5 MHz and the maximum peak power of 1 MW. The antenna is a circular array with an aperture of 8330 m^2. The one-way antenna beam width is 3.6 degree (Fukao et al., 1985). In order to observe meteor head echo which is able to obtain information of the orbit, a special set-up for meteor head echo mode has been developed (Sato et al., 2000 ; Nishimura et al., 2001). Inter-pulse period (IPP) and pulse width are 5.12 ms and 256 μs, respectively. Mono-pulse interferometric method is used for the meteor orbit determination. Orbit of meteors with magnitudes as faint as +15 could be observed with an accuracy of 0.5 degree of radiant direction with this mode (Nishimura et al., 2001). Fig. 2 shows an example of the radar observation result. Echo intensity, Doppler velocity and range are measured by each pulse (every 5 ms), and height and meteor head velocity are further determined for each pulse period.

2.3 Simultaneous observation

Simultaneous observations of faint meteors by the MU radar and the high sensitive video camera system were carried for 9 nights (1150 min) in 2001. First, the radar signals were analyzed with the method developed by Nishimura et al. (2001), and time and direction of meteors were listed. Then, the video tape of the corresponding time was carefully examined, and direction and optical magnitude of meteor head were measured for each video frame. We could obtain 82 simultaneous meteors. The magnitudes of observed meteors were between +3.9 and

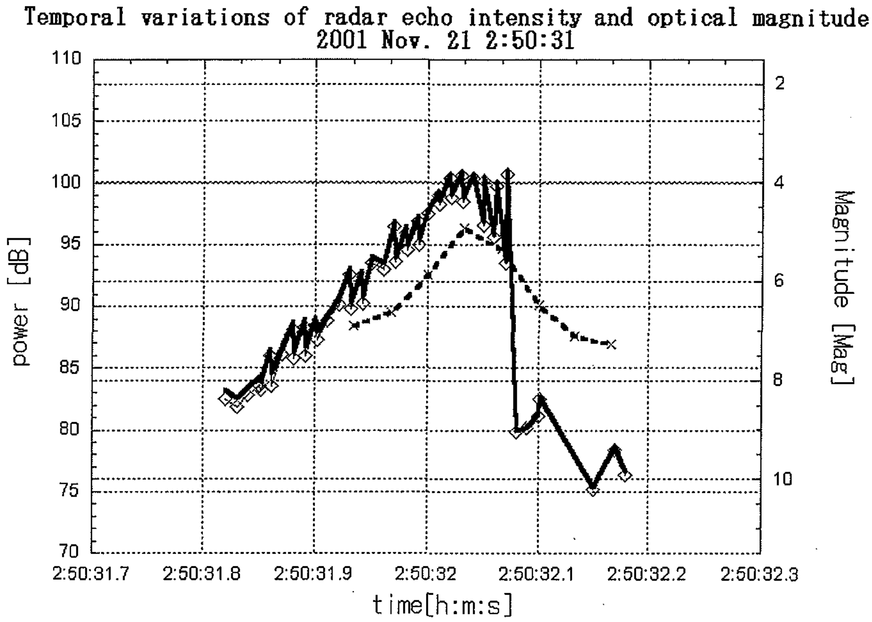

Fig. 3: Time variation of radar echo intensity and optical magnitude of the meteor observed at $2^h50^m31^s$ JST on November 21, 2001. The open diamond shows observed echo intensity. The solid line shows the radar echo intensity with the antenna gain pattern corrected. The dotted line is absolute magnitude observed by the ICCD camera.

+9.1 for lens 1, and between +5.4 and +8.1 for lens 2, respectively. In this study, 26 meteors, of which the time for both radar and optical measurements were successfully synchronized, have been closely analyzed among 82 simultaneous meteors.

3. RESULTS

3.1 Comparison of radar echo intensity and optical magnitude

We investigated temporal variations for 21 meteors by excluding 5 meteors with a larger estimation error due to very large (>30 dB) correction of the antenna gain. Fig. 3 shows an example of time variation of radar echo intensity and absolute optical magnitude of the observed meteors, where the vertical scale is adjusted so that 4 dB in radar intensity corresponds to one optical magnitude. The radar echo intensities are normalized using the range of 100 km. In Fig. 3, radar echo intensity (the antenna gain pattern corrected) increased from 91 dB to 101 dB between $2^h50^m31.920^s$ and 32.020^s, which corresponds to +10 dB/100 ms. It decreased by about 20 dB rapidly at $2^h50^m32.072^s$, and then decreased gradually. The optical magnitude also increased between $2^h50^m31.933^s$ and 32.033^s like the radar echo intensity (2.5 magnitude/100 ms), and reached the maximum magnitude of +4.9 at $2^h50^m32.033^s$, and then decreased gradually but without rapid decrease. Such an example was considered to type I. We classified 26 examples by the characteristics of time variations of radar echo intensity into

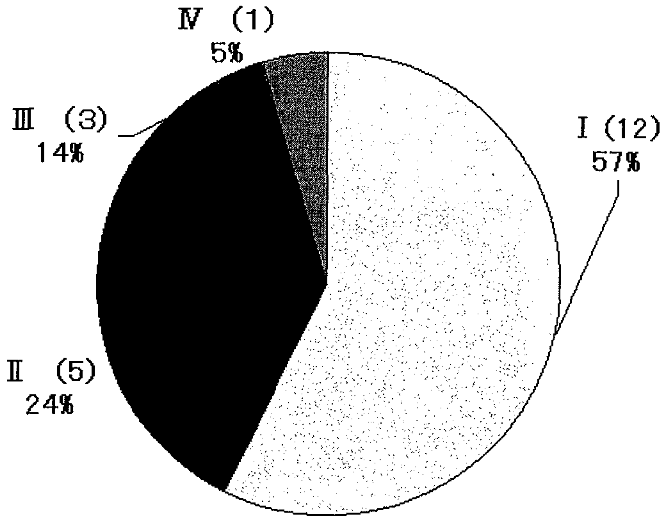

Fig. 4: Classification of observed meteors according to the temporal variations of radar echo intensity. Type I and II shows meteors with a rapid decrease of radar echo intensity by more than 10 dB and by less than 10 dB, respectively. Type III corresponds to meteors with gradual decrease of radar echo intensity (with antenna gain pattern corrected). Type IV denotes meteors with rapid increase of radar echo intensity. Five meteors with a significantly large correction of antenna gain pattern were not used in this classification.

4 types.

Fig. 4 shows the numbers of meteors of different variation patterns (types I - IV). Consequently, we observed 17 meteors with the rapid radar echo intensity decrease by 5 to 30 dB (type I - II), which were 81 % of 21 examples. The magnitude of such rapid decrease of radar echo intensity was 14 dB in average.

3.2 Scatter diagram of radar echo intensity and optical magnitude

Fig. 5 shows the scatter diagram of the radar echo intensity and optical magnitude for 26 examples of the observed meteor. The radar echo intensities were averaged for 1/30 seconds (6 pulses) corresponding to the time resolution of the optical magnitude. The absolute radar echo intensities in the current study and Nishimura et al. (2001) are not calibrated, and therefore the difference (offset) of radar echo intensity is not discussed here. For example, the optical magnitude of the meteors plotted with closed diamond symbols in Fig. 5 changed between +5.4 and +3.6, and the corresponding radar echo intensity changed from 112 dB to 114 dB, indicating the inclination of −2 dB/magnitude. For the meteor brighter than +7 optical magnitude, the inclinations were −1 to −5 dB/magnitude, and suggest that there are positive correlations between radar echo intensity and optical magnitude. Moreover, this result is in agreement with

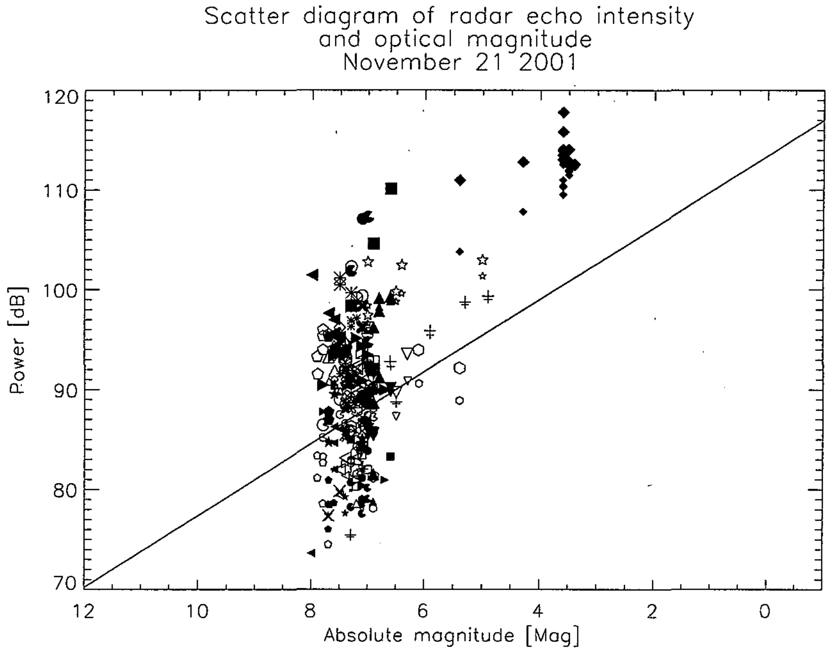

Fig. 5: Scatter diagram of instantaneous (1/30 sec average) radar echo intensity and optical magnitude. The data for the same meteors are plotted with the same symbols. The small symbols show observed echo intensity. The large symbols show the radar echo intensity with the antenna gain pattern corrected. Data with beam pattern correction larger then 30 dB are removed. The solid line indicates the relation obtained by Nishimura et al. (2001).

the result described in Nishimura et al. (2001) (−3.6 dB/magnitude). It is noteworthy that the inclination for the above mentioned meteors shown here is temporal variation for a single meteor, and the results in Nishimura et al. (2001) are the distribution of peak radar echo intensity and peak optical magnitude for many meteors observed at different time. Thus, for our observation with precise time synchronization revealed the relation of optical magnitude and radar echo intensity as a temporal variation of instantaneous values for the same meteors. The distribution of optical magnitude and radar echo intensity at the optical magnitude fainter than +7 magnitude seems to have very large inclination. However, this is probably due to the rapid change of radar echo intensity discussed later.

4. DISCUSSION

A rapid decrease of radar echo intensity was observed for 17 cases out of 21. We excluded 7 samples with short periods of simultaneous observation, and compared the rest 10 cases for further comparison of time variations of radar echo intensity and optical magnitude. For all the cases, the variation of optical magnitude was not larger than 2 (or 8 dB), which was smaller compared with the variation of radar echo intensity. It is also noteworthy that a rapid decrease was not observed for the optical magnitude in any of the 10 cases. Therefore, it is not probable that the energy of the meteor head consumed for ionization and luminosity changed rapidly at the time of rapid decrease of radar echo intensity. The rapid change of radio scatter mechanism

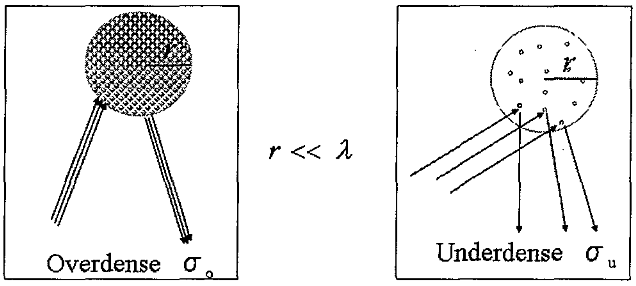

Fig. 6: Simplified model of radio scattering for overdense (left) and underdense (right) head echoes. Note that the radius of the meteor head, r, is assumed to be much smaller than the radar wave length, λ.

is more likely for the reason of the observed time variations.

Here, we assume that the observed change of radar echo intensity was due to the transition between the two scattering mechanics of overdense and unerdense echoes. The former is a total reflection at the surface of critical electron density in a plasma, whereas the latter is the scatter from each free electron in a plasma. Fig. 6 shows a simplified model of such a meteor head with an electron density around the transition. The plasma of the meteor head is assumed to be spherical with a uniform volume electron density, N. The radius of the sphere, r, is assumed to be significantly smaller than the radar wavelength, λ. The RCS (radar cross section) of overdense echo, σ_o, for the spherical meteor head show in Fig. 6 is

$$\sigma_o = \frac{144\pi^5 r^6}{\lambda^4} \tag{1}$$

On the other hand, the RCS for the underdense echo, σ_u is

$$\sigma_u = (\frac{4}{3}\pi r^3 N)^2 \sigma_e \tag{2}$$

where, σ_e is the RCS of a single electron. The electron density, N, at the transition should be equal to the critical electron density of a plasma, and therefore

$$\begin{aligned} N &= (2\pi)^2 f_p^2 \frac{\epsilon_o m}{q^2} \\ &= 2.7 \times 10^3 \qquad [m^{-3}] \end{aligned} \tag{3}$$

where, f_p, ϵ_o, m, and q are plasma frequency, dielectric constant, electron mass and electron charge, respectively. Taking the ratio of (1) and (2) using (3), the RCS ratio at the transition between overdense and underdese echo, σ_o/σ_e becomes independent on the assumed radius of meteor head, r, and a constant value of 13 dB. This ratio is consistent with the results that rapid decrease of the radio echo intensity by 5 - 30 dB (14 dB in average) was frequently observed in our experiment.

Scatter diagram of the radar echo intensity and optical magnitude, Fig. 5, showed that at the magnitude brighter than +7, the inclinations were -1 to -5 dB/magnitude with clear positive correlation. However, in the region with the magnitude fainter than +7, decrease of the radar echo intensity is significantly large. This is probably due to the transition between overdense and underdense region as mentioned above. The inclination at the underdense region is not clear from the Fig. 5, which could be derived to be −8 dB/magnitude from Eq. (2). In order to investigate such a relation we need a more sensitive optical measurement, in future. It should be noted that the difference of radar scattering mechanism between bright and faint meteors, as shown here, should be considered when estimating the mass of meteors, or the optical magnitude from the radar echo intensity of the meteor head echoes.

5. FUTURE WORKS

The future works to be done are

1. A more precise determination of radar echo direction (better estimation of RCS) by calibration of the phase difference of the receiver channels.
2. In order to clarify the relation between the echo intensity and magnitude of faint meteors, extension of the database for fainter meteors than +7 magnitude.
3. Investigates about transition of the head echo from overdense scattering to underdense scattering in more detail.

ACKNOWLEDGMENTS

The authors thank to Mr. Masayoshi Ueda of the Nippon Meteor Society for his help on the data analysis of optical observation. The MU radar belongs to and is operated by Radio Science Center for Space and Atmosphere, Kyoto University.

REFERENCES

Ceplecha, Z., Borovička, J., Elford, W. G., Revelle, D. O., Hawkes, R. L., Porubčan, V., Šimek, M., 1998, Space Science Reviews, vol. 84, pp. 327.
Fukao S., Sato T., Tsuda T., Kato S., Wakasugi K., Makihira T., 1985, Radio Sci. vol. 20, no. 6, pp. 1155.
Nishimura K., Sato T., Nakamura T., Ueda M., 2001, IEICE Trans.Commun. vol. E84-C, no.12, pp. 1877.
Sato T., Nakamura T., Nishimura K., 2000, IEICE Trans.Commun. vol. E83-B, no.9, pp. 1990.
Skolnik, M.I., 1990, Radar Handbook, McGraw-Hill, 2nd Ed., pp. 1200.